Interactions between Caffeine, Theophylline and Derivatives with Gold Nanoparticles and Implications for Aptamer-Based Label-Free Colorimetric Detection

Sarah R. Labas and Prof. Dr. Juewen Liu*

Department of Chemistry, Waterloo Institute for Nanotechnology, University of Waterloo, 200 University Avenue West, Waterloo, Ontario N2L 3G1, Canada

E-mail: liujw@uwaterloo.ca

Abstract

Caffeine, theophylline, and other methylxanthines have interesting biological activities and are consumed in high quantities globally, causing health and environmental concerns. Gold nanoparticles (AuNPs) have excellent optical properties for biosensor development, although little is known about the adsorption of these xanthine derivatives to AuNPs. In this work, interactions of these compounds with AuNPs were studied. Caffeine, theophylline and theobromine are adsorbed in a manner that affords protection against salt-induced aggregation, whereas xanthine and paraxanthine are adsorbed to destabilize and thus aggregate the AuNPs. Caffeine and theophylline are able to protect AuNPs starting at concentrations as low as 6.3 μM. Xanthine and paraxanthine induce significant aggregation at 5 μM. Adsorption was also confirmed by surface-enhanced Raman scattering (SERS). Using two recently selected DNA aptamers for caffeine and theophylline, the label-free colorimetric sensing method was tested; our results indicated that due to adsorption of these target molecules, this method cannot be directly used for their detection. The adsorption of these compounds to AuNPs may enable various detection methods such as SERS, but at the same time, it may complicate other detection methods.

Introduction

Caffeine is a very important molecule due to its widespread consumption.[1] It is extensively and readily available and is the most widely used psychoactive substance. The widespread consumption of caffeine has caused concentrations to rise in the environment and aquatic ecosystems. Although negative effects on humans have not been a major concern, there are reports of possible negative effects on coastal ecosystems.[2] For physiological and environmental reasons, its detection and quantification is an area of growing interest.[3-6]

The chemical name of caffeine is 1, 3, 7-trimethylxanthine, where removing any of the methyl groups generates three new molecules named theophylline, theobromine and paraxanthine, respectively. Theophylline is a main active component in tea, and it has been used to treat airway diseases such as asthma.[7] A lot of efforts have been made pertaining to the detection and quantification of theophylline, especially in blood, due to its pharmaceutical relevance.[7-9]

Our lab recently reported a series of DNA aptamers that can bind caffeine[5] and theophylline,[10] respectively. These aptamers can be used to develop biosensors for selective detection of these molecules. Gold nanoparticles (AuNPs) have been very popular in developing aptamer-based biosensors because of their excellent optical properties.[11-17] Many sensors were designed by taking advantage of the protective effect of aptamers against salt-induced aggregation of AuNPs.[18-19] Aptamer binding to its target was also believed to inhibit aptamer adsorption to AuNPs, and thus AuNPs are easily aggregated upon adding salt.[20-23] The color change due to AuNP aggregation can thus indicate the presence of target analytes. This method hinges on the idea that of the components in the sensor, only DNA aptamers can provide stability against salt-induced AuNP aggregation, and only salt can induce aggregation.

However, we recently discovered that the adsorption of many target analytes to AuNPs needs to be considered.[24] Ignoring such an interaction has led to false positives (seeing aptamer binding where none exists) if aggregation is induced by the target.[25-26] False negatives are also possible, wherein no aggregation is occurring regardless of whether the aptamer is binding to the target, because excess target is protecting AuNPs against salt-induced aggregation.[27-28]

The adsorption of caffeine, theophylline and other methylxanthines on silver nanoparticles was studied in previous works, though the adsorption of these molecules on AuNPs has yet to be reported.[29-31] We herein systematically studied the adsorption of caffeine, theophylline and

related compounds to gain fundamental insights. We also tested the AuNP-based detection method and concluded that this method cannot be directly used for the detection of caffeine or theophylline due to the adsorption of these molecules onto AuNPs.

Results and Discussion

Colloidal stability of AuNPs in the presence of caffeine and related compounds. The structures of caffeine and related compounds tested in this work are shown in Figure 1. Each of these structures consists of the same xanthine core with different numbers of methyl groups. Freely dispersed AuNPs are red in colour. When they become aggregated, their visual appearance shifts to a purple or blue color. For the as-synthesized citrate-capped AuNPs, and the AuNPs with added caffeine, theophylline, and theobromine, we saw an identical red colour, indicating that these molecules did not induce aggregation (Figure 1). This differs from the purple and blue color that resulted upon the addition of paraxanthine and xanthine, respectively, which are indicative of aggregation of our AuNPs.

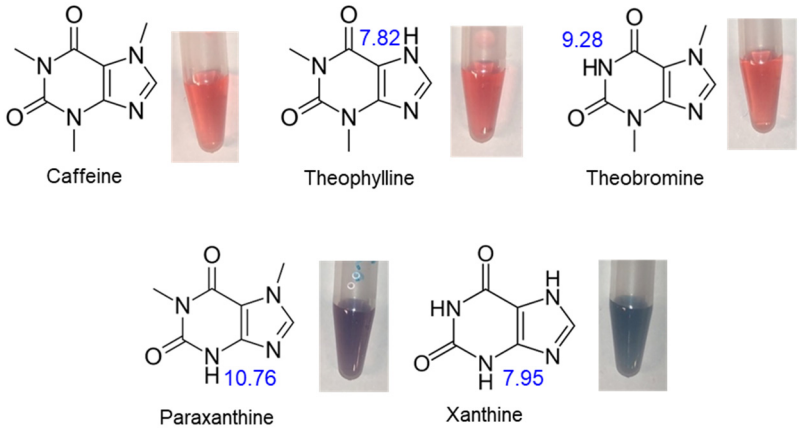


Figure 1. The structure of caffeine and its derivatives, and photographs of AuNPs following the addition of caffeine, theophylline, theobromine, paraxanthine and xanthine, respectively. Samples have final concentrations of 4.6 nM AuNPs, 2.5 mM MES buffer, pH 6.1 and 500 µM target. pK_a values are shown in blue, next to the proton that they correspond to. All pK_a values given were taken from their respective PubChem compound summary sheets.[32]

This color change also shifted the wavelength at which maximum absorbance is observed. Freely dispersed AuNPs absorb maximally around 520-525 nm, and aggregated AuNPs absorb over a wider range, around 600-700 nm. To quantify the color, UV-vis spectroscopy was used, and absorbance ratios (620 nm/523 nm) were determined. Given that aggregated AuNPs absorb higher at 620, and freely dispersed AuNPs absorb more at 523, high absorbance ratios indicate that the AuNPs are aggregated, and low ratios are indicative of freely dispersed AuNPs.

Since adenosine-induced aggregation of AuNPs has been well studied,[27, 33] we also included adenosine and adenine in this experiment for comparison. Adenosine-induced aggregation is evidenced by the increasing ratio of absorbance as the concentration of adenosine increases, with aggregation starting at very low concentrations (Figure 2A). The fitting shown in Figure 2A for adenosine resulted in an apparent K_d of adenosine to AuNPs of 7.2 µM. To contrast this, as the concentrations of both caffeine and theophylline were increased to even 500 µM, the ratio of absorbance remained low and comparable to that of the pure AuNPs, which is indicative of a lack of aggregation.

In contrast, xanthine and paraxanthine showed increasing ratios of absorbance as the concentrations of these targets increased (Figure 2B). Both targets can readily induce aggregation starting at low micromolar concentrations and reach a plateau at approximately 5 µM. Theobromine is comparable to caffeine and theophylline in that increasing the concentration has no significant effect on the absorbance ratio, suggesting that theobromine cannot induce aggregation.

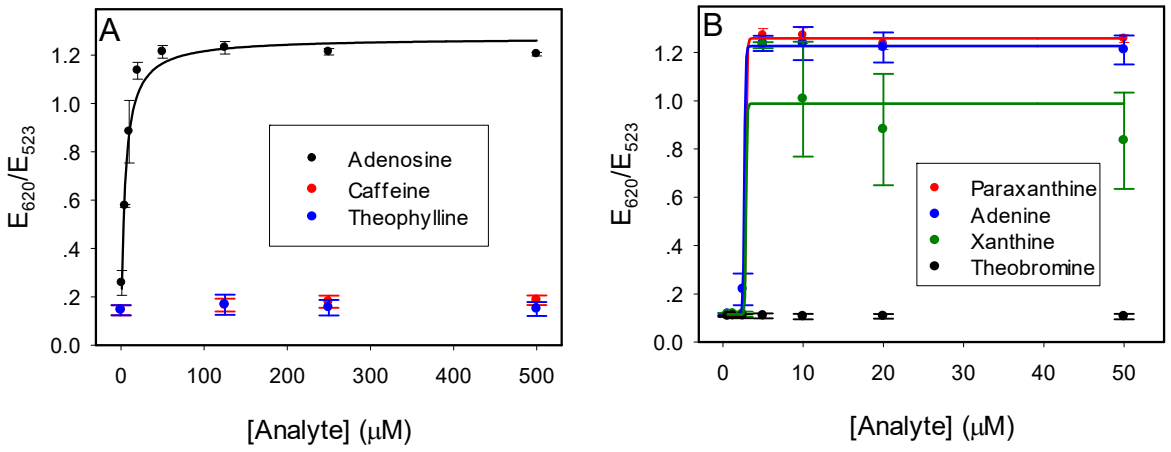


Figure 2. (A) The extinction ratio of the AuNPs in the presence of caffeine, theophylline, and adenosine. Adenosine was included as a positive control. (B) The extinction ratio of the AuNPs in the presence of paraxanthine, theobromine, xanthine, and adenine. Experiments were repeated in triplicate.

Protection of AuNPs by caffeine and theophylline indicative of adsorption. Given that no target-induced aggregation was observed for either caffeine or theophylline, it was unclear whether these two molecules can be adsorbed to AuNPs. To test this, we then determined whether these two molecules would protect AuNPs against salt-induced aggregation. To ensure that any protection observed can be afforded to the presence of the target of interest, no buffer was included in these methods. Samples were prepared using AuNPs, target and NaCl exclusively.

For both caffeine and theophylline, increasing their concentration decreased the absorbance ratios (Figure 3A). Thus, we can conclude that they protected AuNPs against salt-induced aggregation. Protection plateaus at approximately 125 μM for both caffeine and theophylline, with noticeable protection being observed starting at 6.3 μM for both studied targets. Such protection was indicative of adsorption of these two molecules to AuNPs. The effect of pH on the protection afforded by theophylline was also studied. Both acidic (pH 4.2) and basic (pH 10.2) conditions were assayed. These experiments showed an increase in protection at low concentrations of theophylline at pH 10.2, and a slight decrease in protection at the lowest concentrations of theophylline at pH 4.2 (Figure S3). Protection remained comparable at concentrations greater than 6.3 μM for each reaction condition. These results indicated that pH does not have a notable impact on the protection offered by theophylline. The NaCl control (no theophylline) at pH 10.2 also had a slightly decreased ratio of absorbance. Thus, the pH 10.2 buffer itself may be contributing to the slight increase in protection shown in Figure S3.

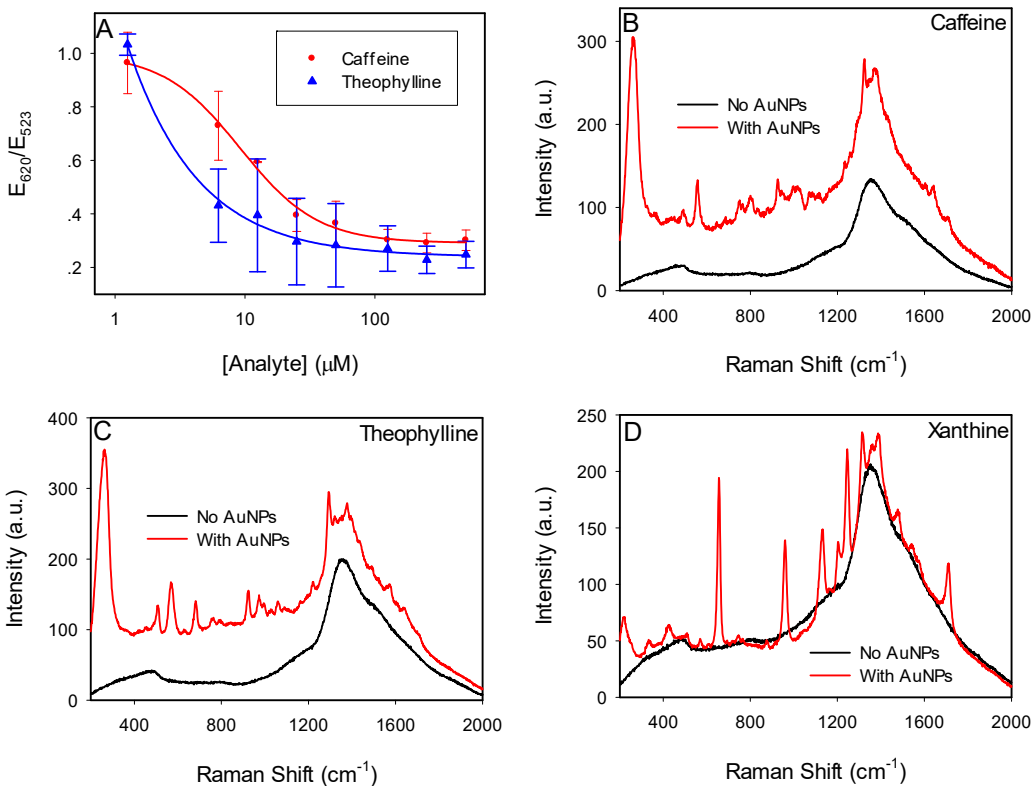


Figure 3. (A) Protection of AuNPs offered by caffeine and theophylline. Samples were prepared using 3 nM AuNPs with a final of 40 mM NaCl added. SERS spectra of (B) 5 mM caffeine alone, and 0.5 mM caffeine with 100 nm AuNPs and 1.2 mM $MgSO_4$, (C) 0.5 mM xanthine alone, and 0.05 mM xanthine with 100 nm AuNPs and 1.2 mM $MgSO_4$, (D) 5 mM theophylline solution, and 0.5 mM theophylline with 100 nm AuNPs and 1.2 mM $MgSO_4$.

When comparing the structures of caffeine and its derivatives (Figure 1A), there is a notable difference between the compounds that can induce aggregation and those that do not. It is tied to the presence versus absence of a methyl-capped nitrogen in the N3 position. The N3 methyl-cap is missing on xanthine and paraxanthine and these are the only caffeine derivatives studied here that induced aggregation. Caffeine, theophylline, and theobromine are methyl-capped on this nitrogen, and none of these compounds induced aggregation of the AuNPs. Given this, we reasoned that the structures of the targets being studied are critical in determining whether an interaction would stabilize or destabilize AuNPs. Note that they were all adsorbed to the AuNPs.

The charge of a molecule is known to strongly influence its ability to stabilize AuNPs. For example, adenosine destabilizes AuNPs, while ATP stabilizes them, since the latter has a negatively charged triphosphate.[27] At our experimental condition pH of 7.3, each of these molecules exists in a neutral charge state (0 formal charge). With this, the pK_a values of these molecules (shown in Figure 1) do not seem to be an important parameter for determining whether a target may have a stabilizing or destabilizing effect on AuNPs.

A possible explanation for the lack of methyl cap contributing to aggregation is that this N3 position can coordinate to the AuNP surface to help displace the surface citrate, resulting in a more charge neutral surface. Alternatively, if this position is not adsorbed, it may serve as a hydrogen bond donor to interact with a ligand on another AuNP to induce aggregation. These roles either decrease charge repulsion or increase inter-particle attraction, both promoting AuNP aggregation.

SERS to study adsorption. For both stabilization and destabilization interactions, the likely cause is the adsorption of the target onto the AuNPs. To further verify adsorption, surface-enhanced Raman scattering (SERS) was performed for caffeine, theophylline, and xanthine (Figures 3B-D). Compared to the free molecules in water, the SERS samples with AuNPs had much stronger signals despite their concentrations being 10-fold lower, confirming adsorption. The Raman spectra obtained were consistent with literature values for xanthine peaks. In work done by Muniz-Miranda to study xanthine using Raman spectroscopy and silver nanoparticles, enhanced peaks at around 657 cm^{-1} were observed.[31] In Figure 3C, we also observed a strongly enhanced peak at approximately 657 cm^{-1}, which solidly suggested adsorption of xanthine onto the AuNPs. The Raman spectra for caffeine also suggested absorption, which is given by the enhanced peak at approximately 555 cm^{-1} (Figure 3B).[29] Theophylline results are indicative of adsorption as well, as evidenced by the peaks at 555 cm^{-1} and 1570 cm^{-1} (Figure 3D).[30] These results strengthened our hypothesis, supporting that the stabilization or destabilization interactions with AuNPs were afforded due to the adsorption of our targets onto the AuNPs.

Protection of AuNPs by the aptamers. For the sensing method to work as intended, aptamers must be able to protect the AuNPs against salt-induced aggregation. Figure 4A and 4B illustrate the predicted secondary structures of the caffeine and theophylline aptamers, respectively. To ensure that the aptamers were suitable for the sensing method, preliminary experiments were done

to verify the protection. As the concentration of the aptamer increased, the ratio of absorbance decreased proportionally (Figure 4C), confirming that these aptamers can indeed protect the AuNPs. Protection was observed at each of the studied concentration to varying degrees. Protection reached a plateau at around 100 nM, for both the caffeine and theophylline aptamers. Given these results, 100 nM aptamer concentrations were used for subsequent experiments.

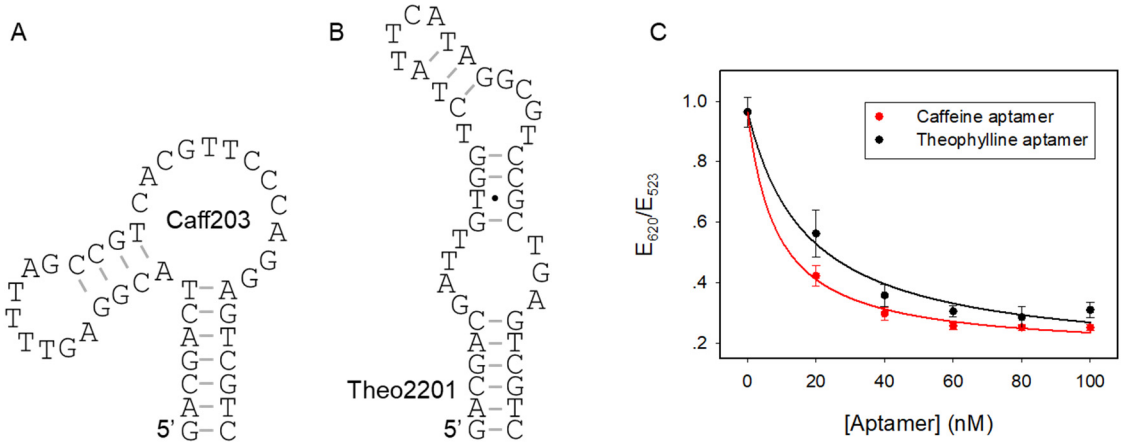


Figure 4. The secondary structure of the (A) caffeine and (B) theophylline aptamers. (C) Protection against salt-induced aggregation offered by caffeine and theophylline aptamers.

Label-free colorimetric sensing of caffeine and theophylline. Single-stranded DNA molecules can interact with the surface of AuNPs in a way that stabilizes the AuNPs. This interaction is due to the nitrogenous lone pairs that are present on nucleobases. NaCl destabilizes AuNPs by screening the surface charge, such that aggregation ensues. The typically proposed sensing mechanism makes use of these two interactions to determine whether an aptamer sequence is binding to a particular target. Specifically, when both DNA and NaCl are present, the protective, or stabilizing, effect of DNA is dominant, and thus the AuNPs are protected against salt-induced aggregation. However, when the target of said aptamer is included in the system, the aptamer will preferentially interact with the target, thus reducing or eliminating the protective effect of the aptamer for the AuNPs (Figure 5A).

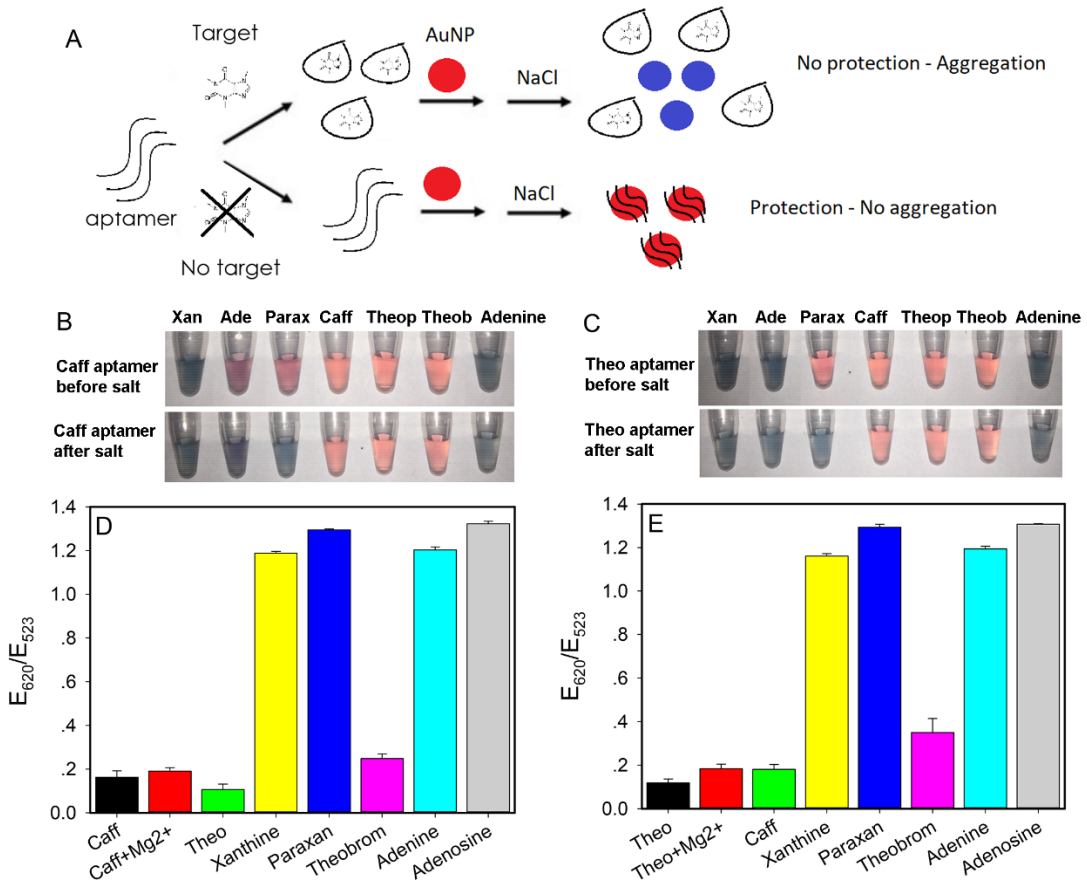


Figure 5. (A) The conventional mechanism for the label-free sensing method. In this mechanism, only the adsorption of aptamers is considered, while the adsorption of target molecules is not considered. Photographs of sensing results using the (B) caffeine aptamer and (C) theophylline aptamer before and immediately after adding NaCl. Samples consisted of 1 mM phosphate buffer, pH 7.3, 4 nM AuNPs, 10 μM target, 100 nM DNA aptamer, and 0 or 40 mM NaCl. Quantified sensing assay results with caffeine (D) and theophylline (E) aptamers after adding 40 mM NaCl. For the samples with Mg^{2+} added, 0.5 mM Mg^{2+} was used.

Following the method in Figure 5A, we tested the detection caffeine and its derivatives using the caffeine and theophylline aptamers. Given that in the samples shown in Figure 5B and 5C, NaCl had thus far not been added, yet aggregation was observed for some molecules, it becomes evident that the target-AuNP interaction was predominating in those cases. If DNA-AuNP were the primary interactions in the system, there would be no aggregation before the

addition of salt. Aggregation prior to salt addition means that the target can induce aggregation of the AuNPs regardless of the presence of aptamers.

As further evidence for the dominance of the target-AuNP interaction, neither caffeine with the caffeine aptamer (Figure 5D), nor theophylline with the theophylline aptamer (Figure 5E) samples showed aggregation upon the addition of salt. This again shows that it is the target that is interacting with AuNPs more strongly, as no aggregation is observed where it is expected to occur due to the protection against salt-induced aggregation offered by caffeine and theophylline. For each of the samples shown in Figures 5B-E, aggregation is shown to be based on the interaction of the target with AuNPs (i.e., those targets that were shown to induce aggregation in previous assays are again showing aggregation in the sensing experiment here, and those that were shown to offer protection against salt-induced aggregation in previous assays are showing no discernable change in absorbance ratio following the addition NaCl).

Further tests were done to assess whether a higher concentration of salt may alter the results. Concentrations up to 100 mM NaCl were assayed (Figure S1). These assays showed that the sensing result was dependent on the presence versus absence of theophylline – assays were done with just theophylline, theophylline and aptamer, and just aptamer (each with NaCl and AuNPs). For each assayed concentration of salt, the sensing results mirrored the theophylline-only result, suggesting that the theophylline-AuNP interaction is dominant in the system, regardless of the NaCl concentration used. Even more, $MgCl_2$ was added to the caffeine aptamer sample to promote aptamer-target binding. However, despite adding $MgCl_2$, still no aggregation was observed for the caffeine with caffeine aptamer sample (Figure 5D). The same can be said for the sensing assay with the theophylline and theophylline aptamer, which also included 0.5 mM $MgCl_2$ (Figure 5E). Increasing $MgCl_2$ further was not possible, as higher concentrations of Mg^{2+} can readily induce aggregation of the AuNPs.

Therefore, based on this sensing assay, this system was dominated by target/AuNP interactions. If the DNA-AuNP interaction dominates, the samples with targets that do not bind the aptamer should not show any aggregation, and the targets which bind to the aptamer will show aggregation once NaCl had been added. If the target-gold interaction dominates, then aggregation will depend solely on the stabilization/destabilization interaction of the target with AuNPs. Prior to adding NaCl, aggregation is already seen in the samples with xanthine, adenosine, and adenine.

Because the paraxanthine samples aggregated slower than other aggregation-inducing targets, paraxanthine kinetics experiments were done (Figure S4). These experiments showed that aggregation began between 5-10 min after adding paraxanthine to the AuNPs, and full aggregation (E_{620}/E_{523} >1.0) was reached at approximately 30 min.

Based on whether target molecules can adsorb and whether DNA can bind to target, there are four possibilities as summarized in Figure 7. In Figure 7B and 7D, we are getting the 'expected' result – aggregation when target of interest is present, and no aggregation when a non-target is present. However, despite these being the expected results, the underlying mechanism can be different from previously reported. Previous iterations of this sensing method conclude that aggregation occurs because no protection against salt-induced aggregation is being afforded by DNA, when in-fact we would see aggregation prior to adding salt. This indicates target-induced destabilization of the AuNPs (as suggested in Figure 7D). As well, there is potential for both false-negative and false-positive results, as shown in Figure 7A and 7C. In Figure 7A, despite there being DNA-target binding, no aggregation is observed because of the stabilization effect of the target. The conclusion would be that no binding is occurring, when in fact it is simply being masked. Alternatively, Figure 7C shows a false-positive – it appears as though binding is occurring, though aggregation ensues before salt addition because of the destabilizing effect of the target.

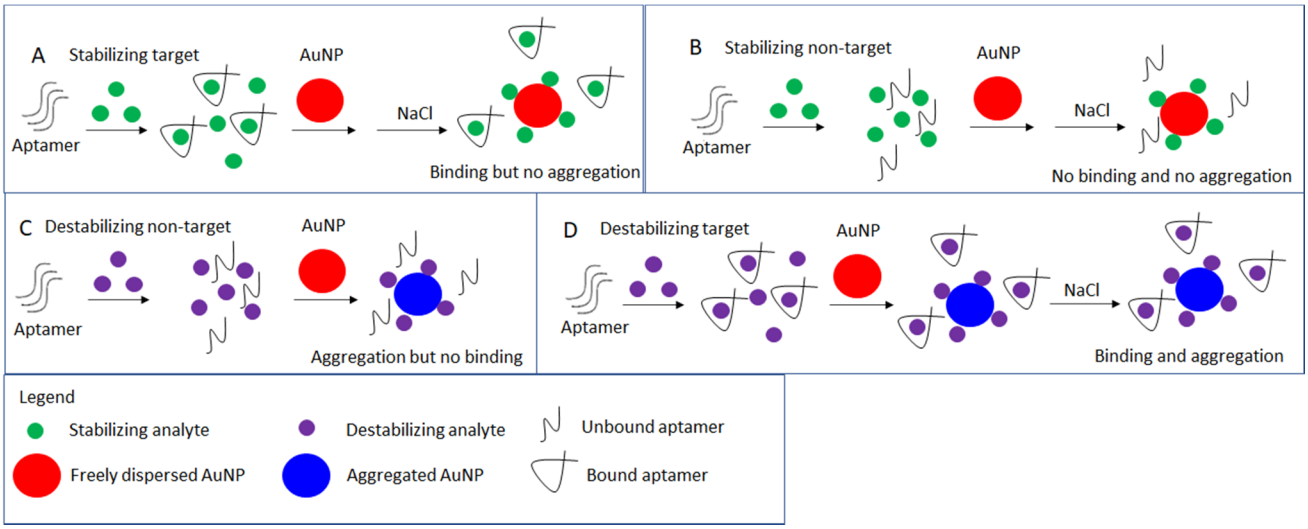


Figure 7. Possible results for the sensing assay when the target is dominating in the system. (A) The expected results when a stabilizing target is used. (B) The expected results when a stabilizing

non-target is assayed. (C) The expected result when a destabilizing non-target is used, and (D) the expected result when a destabilizing target is assayed.

Considering results reported here, and the described potential results, previous work that made use of this method may need to be revisited to ensure the validity of the conclusions. For instance, this method has been used as proof of successful aptamer selection for a number of sequences.[34] Because of the stringency required for success, these sequences may need to be studied using alternate methods to ensure their viability. An example where the constraints not being met did in fact lead to false conclusions is shown in work done by Zong *et al*.[35] This false conclusion came about partially due to the failure to report target-gold interactions between arsenic and AuNPs.[36]

For this method to be successful as it has been intended,[24] three primary constraints should be met: 1) NaCl must be the only component in the system which can induce the aggregation of AuNPs; 2) the DNA aptamer must be able to protect against salt-induced aggregation, and it must be the only component in the system which can do so; 3) the target in question must not interact with AuNPs in either a stabilizing nor a destabilizing manner. If such an interaction were to exist, it must be weaker than the interaction of DNA with AuNPs.

Conclusions

In this work, we studied the adsorption of caffeine and theophylline by AuNPs and evaluated the feasibility of aptamer-based label-free detection. Adsorption was observed based on the colloidal stability of AuNPs and Raman spectroscopy, and due to such adsorption, the AuNPs could not be used for direct label-free colorimetric detection. Future research on more reliable methods for detection and quantification of small molecules using AuNPs would need to carefully consider target-gold interactions. Alternate methods with less constraints for success can be explored. Results presented in these works also suggest that the method as reported should not be used as proof of aptamer binding, and alternate binding assays should be employed when reporting new aptamer sequences.

Experimental Section

Chemicals. The 13 nm AuNPs were used for all assays other than Raman spectroscopy. The 13 nm AuNPs were prepared according to literature.[37] A 1 mM $HAuCl_4$ solution was heated to refluxing, and then a 1% $Na_3C_6H_7{\cdot}2H_2O$ was added to the refluxing solution. This was allowed to react until a wine-red color was achieved; the solution was then slowly cooled. DNA samples were purchased from Integrated DNA Technologies (Coralville, IA, USA). The caffeine aptamer sequence is 5′-GAC GAC TAC GGA GTT TTA GCC GTC ACG TTC CCA GGA GTC GTC-3′, and the theophylline aptamer sequence is 5′-GAC GAC GAT TGT GGT CTA TTC ATA GGC GTC CGC TGA GTC GTC-3′. Sodium chloride, 4-(2-hydroxyethyl) piperazine-1-ethanesulfonic acid (HEPES), MES, NaH_2PO_4, Na_2HPO_4, KH_2PO_4, caffeine, theophylline, xanthine, paraxanthine, theobromine, adenine and adenosine were purchased from Sigma-Aldrich. Milli-Q water was used to prepare all the solutions and buffers.

AuNP stability assays. To assess the effect of the target molecules on the stability of the AuNPs, titrations were made to a final concentration of 3 nM AuNPs, and target concentrations ranged from 1 μM to 2 mM. Reactions consisted of 55 μL of AuNPs and 55 μL of respective target solution. For consistency, samples were allowed to sit for 1 h at room temperature before measurements were taken on a UV-Vis spectrophotometer. For pH studies, a carbonate/bicarbonate buffer was used for pH 10.2, and a sodium phosphate/potassium phosphate buffer was used for pH 4.2.

Aptamer-based sensing Protection offered by the chosen aptamer sequences was first assessed by aggregation experiments. An approximately 4 nM final concentration of AuNPs was used, with aptamer concentrations ranging from 20-100 nM. Samples were made up of 70 μL AuNPs, 10 μL of the respective DNA solution, and 20 μL of NaCl (40 mM final). The sensing experiments were done by first mixing the aptamer with target and were left to interact for 5 min; and a 5 mM phosphate buffer, pH 7.3 was used for this reaction. Next, AuNPs were added, and results were photographed. Finally, NaCl was added to each of the samples and results were again photographed and recorded using UV-Vis spectrometry. The final concentrations of the reactants were 100 nM DNA, 10 μM target molecules, 40 mM NaCl, 1 mM phosphates buffer, and approximately 4 nM AuNP. The final sample volume was 100 μL, which consisted of 60 μL AuNPs, 10 μL aptamer solution, 10 μL target, and 20 μL NaCl. Alternate salt concentrations were

assayed for the sensing experiments with theophylline. 10 μM theophylline, 100 nM theophylline aptamer, and 4 nM AuNP concentrations were used; NaCl concentrations ranged from 40 mM to 100 mM.

SERS and UV-vis Spectroscopy Samples were prepared using 100 nm AuNPs prepared by citrate reduction. The final caffeine, theophylline and xanthine concentrations were 0.05 to 0.5 mM, and 1.2 mM $MgSO_4$ was used when needed, to aggregate the AuNPs to increase Raman hotspots. For the AuNP-free spectra, the concentration of the molecules was 10-fold higher. Measurements were taken using a DeltaNu Advantage 785 Raman spectrophotometer, with an excitation wavelength of 785 nm and an integration time of 5 s. All UV-vis spectrophotometry results were obtained using an HP/Agilent 8453 UV-Vis spectrophotometer.

Acknowledgements

Funding for this work was from the Natural Sciences and Engineering Research Council of Canada (NSERC).

Keywords: aptamers; biosensors; caffeine; theophylline; nanomaterials

References

[1] N. OGAWA, H. UEKI, *Psychiatry Clin. Neurosci.* **2007**, *61*, 263-268.

[2] L. R. Vieira, A. M. V. M. Soares, R. Freitas, *Chemosphere* **2022**, *286*, 131675.

[3] L. Svorc, *Int. J. Electrochem. Sci.* **2013**, *8*, 5755-5773.

[4] N. González, S. P. Lantmann Corral, G. Zanini, H. Montejano, C. C. Acebal, *Analyst* **2020**, *145*, 2279-2285.

[5] P.-J. J. Huang, J. Liu, *Anal. Chem.* **2022**, *94*, 3142–3149.

[6] W. Xu, T.-H. Kim, D. Zhai, J. C. Er, L. Zhang, A. A. Kale, B. K. Agrawalla, Y.-K. Cho, Y.-T. Chang, *Sci. Rep.* **2013**, *3*, 2255.

[7] P. J. Barnes, *Pharmaceuticals* **2010**, *3*, 725-747.

[8] S. Feng, C. Chen, W. Wang, L. Que, *Biosens. Bioelectron.* **2018**, *105*, 36-41.

[9] H. Jiang, K. Ling, X. Tao, Q. Zhang, *Biosens. Bioelectron.* **2015**, *70*, 299-303.

[10] P.-J. J. Huang, J. Liu, *ACS Chem. Biol.* **2022**, *17*, 2121-2129.

[11] K. Saha, S. S. Agasti, C. Kim, X. Li, V. M. Rotello, *Chem. Rev.* **2012**, *112*, 2739−2779.

[12] A. B. Chinen, C. M. Guan, J. R. Ferrer, S. N. Barnaby, T. J. Merkel, C. A. Mirkin, *Chem. Rev.* **2015**, *115*, 10530-10574.

[13] B. Liu, J. Liu, *Matter* **2019**, *1*, 825-847.

[14] L. L. Li, H. Xing, J. J. Zhang, Y. Lu, *Acc. Chem. Res.* **2019**, *52*, 2415-2426.

[15] E. M. McConnell, J. Nguyen, Y. Li, *Front. Chem.* **2020**, *8*, 434.

[16] J. L. Chávez, W. Lyon, N. Kelley-Loughnane, M. O. Stone, *Biosens. Bioelectron.* **2010**, *26*, 23-28.

[17] X. Q. Tao, Y. Y. Peng, J. W. Liu, *J. Food Drug Anal.* **2020**, *28*, 575-594.

[18] H. Li, L. J. Rothberg, *J. Am. Chem. Soc.* **2004**, *126*, 10958-10961.

[19] H. Li, L. Rothberg, *Proc. Natl. Acad. Sci. U. S. A.* **2004**, *101*, 14036-14039.

[20] D.-K. Nguyen, C.-H. Jang, *Micromachines* **2021**, *12*, 1526.

[21] Q. u. A. Zahra, Z. Luo, R. Ali, M. I. Khan, F. Li, B. Qiu, *Nanomaterials* **2021**, *11*, 840.

[22] X. Ma, Z. Guo, Z. Mao, Y. Tang, P. Miao, *Microchim. Acta* **2017**, *185*, 33.

[23] N. Katiyar, L. S. Selvakumar, S. Patra, M. S. Thakur, *Anal. Methods* **2013**, *5*, 653-659.

[24] F. Zhang, J. Liu, *Analysis Sensing* **2021**, *1*, 30-43.

[25] X. Liu, F. He, F. Zhang, Z. Zhang, Z. Huang, J. Liu, *Anal. Chem.* **2020**, *92*, 9370–9378.

[26] J. Zhou, Y. Li, W. Wang, Z. Lu, H. Han, J. Liu, *Langmuir* **2020**, *36*, 11490–11498.

[27] F. Zhang, P.-J. J. Huang, J. Liu, *ACS Sens.* **2020**, *5*, 2885–2893.

[28] Y. Hu, Z. Huang, B. Liu, J. Liu, *ACS Appl. Nano Mater.* **2021**, *4*, 1377-1384.

[29] I. Pavel, A. Szeghalmi, D. Moigno, S. Cîntă, W. Kiefer, *Biopolymers* **2003**, *72*, 25-37.

[30] P. Liu, R. Liu, G. Guan, C. Jiang, S. Wang, Z. Zhang, *Analyst* **2011**, *136*, 4152-4158.

[31] F. Muniz-Miranda, A. Pedone, M. Muniz-Miranda, *Acs Omega* **2018**, *3*, 13530-13537.

[32] https://pubchem.ncbi.nlm.nih.gov/ link for the pKa values

[33] B. Liu, P. Wu, Z. Huang, L. Ma, J. Liu, *J. Am. Chem. Soc.* **2018**, *140*, 4499–4502.

[34] K.-M. Song, E. Jeong, W. Jeon, M. Cho, C. Ban, *Anal. Bioanal. Chem.* **2012**, *402*, 2153-2161.

[35] C. Zong, J. Liu, *Anal. Chem.* **2019**, *91*, 10887-10893.

[36] C. Zong, Z. Zhang, B. Liu, J. Liu, *Langmuir* **2019**, *35*, 7304-7311.

[37] J. Liu, Y. Lu, *Nat. Protoc.* **2006**, *1*, 246-252.

ToC Entry

This study is focused on the interaction between gold nanoparticles and two important methylxanthines: caffeine and theophylline. Both molecules adsorb onto gold nanoparticles and protect their colloidal stability, and such adsorption disallows the use of the classic label-free colorimetric sensing method.

